Test Weak Cosmic Censorship Conjecture on Peldan Black Hole Surrounded by Quintessence

Hao TANG(唐浩) *[1,2] and Jia ZHANG(张甲)[1,2]

[1]School of Physics and Electrical Engineering, Weinan Normal University, 714099, China
[2]The Research Center for X Ray Detection and Application of Shaanxi Province, 714099, China

Abstract

We investigate the weak cosmic censorship conjecture (WCCC) for (2+1)-dimensional static Peldan electrostatic black holes surrounded by quintessence. Previous studies have shown that a naked singularity can form in the vacuum Peldan spacetime, potentially violating causality. To examine whether the surrounding quintessence fluid can protect the horizon, we perform a gedanken experiment in which a charged test particle is absorbed by the black hole. We find that although a particle with energy in the formal overcharge window could, in principle, destroy the event horizon, an exterior repulsive potential barrier prevents such particles from ever reaching the horizon. The weak cosmic censorship conjecture therefore remains valid once quintessence is taken into account, consistent with our previous results for the Reissner–Nordström–quintessence case. This suggests that quintessence dark energy may play a protective role in black hole stability, within the physically motivated parameter ranges examined in this work.

Keywords: Peldan black hole; quintessence; weak cosmic censorship conjecture;

PACS numbers: 04.20.Dw, 04.70.Bw, 7.60.Lf

*Corresponding author. E-mail: taho@vip.163.com

1 Introduction

Proposed by Penrose in 1969, the weak cosmic censorship conjecture (WCCC) is a foundational hypothesis of classical general relativity, asserting that all curvature singularities generated by gravitational collapse are permanently concealed behind event horizons, such that naked singularities cannot be observed outside the event horizon[1]. A standard theoretical framework to test WCCC relies on gedanken experiments, in which charged or spinning test particles are used to test the extremal or nearly extremal black holes. Proper charge, energy or angular momentum carried by the test particle may theoretically overcharge or overspin the black holes and erase all real event horizons, leading to observable naked singularities and a violation of WCCC[2].

Many analytical and numerical examinations of WCCC have predominantly focused on various black hole spacetimes, such as the Reissner-Nordström (RN) and Kerr vacuum black holes[3, 4, 5, 6, 7]. Subsequent research extended these thought experiments to black hole geometries embedded in quintessence dark energy backgrounds, motivated by cosmological observations confirming the accelerated expansion of the universe, which requires a dark energy fluid obeying the equation of state $p = \omega\rho$ with state parameter satisfying $-1 < \omega < -\frac{1}{3}$ [8, 9, 10, 11, 12, 13]. For four-dimensional RN-Quintessence(RN-Q) spacetimes, the additional quintessence correction term modifies the radial metric function, shifts the locations of inner and outer horizons, and reshapes the critical energy thresholds separating safe accretion and horizon-destroying overcharge processes [11].

Compared with four-dimensional charged black hole solutions, $(2 + 1)$-dimensional Peldan black holes offer a simplified low-dimensional platform for testing WCCC with electromagnetic charge and dark energy corrections. The Peldan metric incorporates logarithmic radial contributions originating in the $(2+1)$-dimensional Maxwell field, which generate horizon and geodesic behaviors qualitatively distinct from polynomial four-dimensional RN geometries [14, 15]. Ref. [16] suggests that the WCCC might be violated in this geometry. In order to find a possible way to "protect" the black hole, and based on our previous results for the RN-Q case, we consider the Peldan black hole surrounded by quintessence to examine whether a similar protective mechanism holds. This is not only another test of this method, but also an interesting way to test the quintessence model.

A critical technical obstacle differentiating this work from previous RN-Q analyses is the transcendental nature of the Peldan horizon condition. The presence of a logarithmic radial term precludes closed-form elementary analytical expressions for the horizon radii. Furthermore, the vacuum extremal

limit at $\alpha = 0$ corresponds to a double degenerate root of the radial metric function, which renders standard linear perturbative expansions around the degenerate horizon mathematically inconsistent. To avoid the difficulties associated with flawed perturbative methods, we discard analytical approximation and adopt a numerical approach instead.

This paper is organized as follows. Section 2 introduces the full line element of the Peldan spacetime coupled to quintessence fluid, and defines all model parameters. Section 3 derives the covariant conserved energy for radially in-falling charged test particles, constructs the minimal capture energy $E_{\min}$ and maximal overcharge energy $E_{\max}$, and visualizes the overcharge energy window for varying quintessence state parameters. Section 4 numerically solves the transcendental horizon equation for our benchmark parameter set, computes the quintessence modified black hole mass M, and evaluates the radial metric function to demonstrate horizon disappearance after full particle absorption. Section 5 constructs the radial effective potential, locates the exterior repulsive potential barrier via numerical evaluation, and interprets the barrier's dynamical shielding effect for WCCC. Section 6 examines the parameter dependence of this shielding mechanism by performing systematic scans over the quintessence coupling α, the AdS curvature scale l, the black-hole electromagnetic coupling b, and the quintessence state parameter ω. Section 7 summarizes all analytical and numerical results and concludes the paper.

2 Metric of Peldan spacetime with quintessence

We consider the static, circularly symmetric line element describing a (2+1)-dimensional Peldan black hole immersed in a homogeneous quintessence fluid background, written as

$$ds^2 = -F(\rho)dt^2 + \frac{d\rho^2}{F(\rho)} + \rho^2 d\phi^2. \tag{1}$$

The radial metric governing causal structure and horizon locations reads

$$F(\rho) = \frac{\rho^2}{l^2} - 2b^2 \ln \rho - M - \frac{\alpha}{\rho^{2(\omega+1)}}, \tag{2}$$

where l denotes the AdS curvature scale of the three-dimensional spacetime; b is the electromagnetic coupling constant controlling the black hole's inherent charge; M represents the total ADM gravitational mass of the black hole in the presence of non-vanishing quintessence coupling α. The quintessence contribution $-\alpha/\rho^{2(\omega+1)}$ adopted in Eq. (2) follows the (2+1)-dimensional

construction derived in Ref. [17], which provides the three-dimensional generalization of the Kiselev ansatz; where $\alpha > 0$ is the dimensionless coupling strength of the surrounding quintessence fluid, restricted to tiny values $\alpha \ll 1$ consistent with weak dark energy perturbations on astrophysical black holes according to Ref. [18]; ω is the quintessence fluid parameter, constrained to the physical interval $-1 < \omega < -\frac{1}{3}$ to reproduce cosmic accelerated expansion[8].

The static electromagnetic gauge potential sourced by the (2+1)-dimensional Maxwell field follows the standard convention for Peldan geometries:

$$A_t = b \ln \rho, \quad A_\phi = 0. \tag{3}$$

Event horizons of the spacetime correspond to positive real roots of the condition $F(\rho) = 0$. Inspection of Eq. (2) reveals the presence of a logarithmic term $\ln \rho$, which transforms the horizon condition into a transcendental equation with no closed-form elementary analytical solutions for the horizon radii. For this reason, all horizon positions computed within this work are obtained exclusively via numerical methods.

The first radial derivative of the full quintessence-modified metric function $F(\rho)$ is required for extremum analysis of both the spacetime metric and radial effective potential, computed via direct differentiation of Eq. (2):

$$F'(\rho) = \frac{2\rho}{l^2} - \frac{2b^2}{\rho} + \frac{2(\omega+1)\alpha}{\rho^{2(\omega+1)+1}}. \tag{4}$$

The coupled system $F(\rho) = 0$, $F'(\rho) = 0$ defines extremal black hole configurations with quintessence corrections.

3 Conserved energy for radial charged test particle

We consider a massive charged test particle with rest mass m and electromagnetic charge q, undergoing purely radial infalling motion with vanishing angular coordinate velocity $\dot{\phi} = 0$. We adopt the standard numerical simplification $m = E$ universally employed in prior numerical WCCC analyses of vacuum Peldan spacetimes [7, 11, 16]. The spacetime admits a static time-like Killing vector field associated with invariance under time translations, which generates a conserved covariant energy quantity for time-like geodesics. Combining this Killing energy with the minimal electromagnetic coupling to the gauge potential A_t, the total conserved asymptotic energy of

the test particle satisfies[2, 16]

$$E = -qA_t + \sqrt{m^2 F(\rho)\left(1 + \frac{\dot{\rho}^2}{F(\rho)}\right)}. \tag{5}$$

Substituting $A_t = b \ln \rho$ from Eq. (3), we rewrite the full energy-geodesic relation as

$$E = -qb \ln \rho + \sqrt{m^2 F(\rho)\left(1 + \frac{\dot{\rho}^2}{F(\rho)}\right)}. \tag{6}$$

At the outer event horizon location $\rho = \rho_+$, the radial metric function satisfies $F(\rho_+) = 0$, which fully suppresses the square-root kinetic contribution to the conserved energy expression. Rearranging the resulting boundary condition yields the minimal capture energy $E_{\min}$, the threshold energy required for a charged test particle to geometrically reach the outer horizon surface

$$E_{\min} = -qb \ln \rho_+. \tag{7}$$

Eq. (7) shows that $E_{\min}$ depends explicitly solely on the outer horizon radius ρ_+ and the particle charge q, and contains no explicit dependence on the quintessence parameters α and ω. Physically, this is because $E_{\min}$ is fixed entirely by the electromagnetic potential energy $-qA_t$ evaluated at the horizon. The quintessence parameters affect $E_{\min}$ only implicitly, through their influence on the horizon radius ρ_+ determined by $F(\rho_+) = 0$; once ρ_+ is specified, $E_{\min}$ is independent of α and ω. Any test particle with conserved energy $E < E_{\min}$ lacks sufficient radial momentum to make contact with the outer horizon and cannot be fully accreted by the black hole.

For an extremal black hole with mass M_e, following complete absorption of the charged test particle, the black hole's inherent electromagnetic coupling and total gravitational mass are updated to reflect the particle's charge and energy contributions. The accretion parameter shift rules read

$$b \to b + q, \quad M \to M_e + E. \tag{8}$$

The quintessence fluid background remains unmodified by the particle absorption process, so the coupling constants α and ω retain their original values throughout the accretion evolution. The radial metric function Eq. (2) becomes

$$F_{\text{after}}(\rho) = \frac{\rho^2}{l^2} - 2(b+q)^2 \ln \rho - (M_e + E) - \frac{\alpha}{\rho^{2(\omega+1)}}. \tag{9}$$

The event horizon is completely erased from the spacetime if and only if $F_{\text{after}}(\rho) > 0$ for all positive radial coordinates $\rho > 0$, meaning the metric

function never crosses zero to form a real geometric horizon. Setting the minimal value of $F_{\text{after}}(\rho) = 0$ defines the maximal overcharge energy threshold $E_{\max}$, the proper particle energy at which full absorption exactly eliminates all event horizons

$$E_{\max} = \frac{\rho^2}{l^2} - 2(b+q)^2 \ln \rho - \frac{\alpha}{\rho^{2(\omega+1)}} - M_e. \tag{10}$$

If $E_{\min} < E_{\max}$, it implies that there exists an energy gap between $E_{\min}$ and $E_{\max}$. If the test particle carries the energy E that satisfies $E_{\min} < E = m < E_{\max}$, it can fall into the black hole and cause the horizon to vanish.

In order to examine the result, we take a consistent set of parameters $b = 1$, $l = 0.5$, together with a small quintessence coupling $\alpha = 0.0005 \ll 1$, for all numerical evaluations presented in the subsequent sections. For the state parameter we choose $\omega = -0.5$ (the reason for this choice will be discussed below), and for these values the extremal mass evaluates numerically to

$$M_e = 2.38529. \tag{11}$$

All extremal quantities quoted in this work, including M_e and the horizon radii given below, are obtained by numerically solving the coupled system $F(\rho) = 0$ and $F'(\rho) = 0$.

Numerical root-finding applied to the transcendental horizon condition $F'(\rho) = 0$ yields three distinct algebraic radial roots as

$$\rho_1 = -0.500125, \quad \rho_2 = 0.00025, \quad \rho_3 = 0.499875. \tag{12}$$

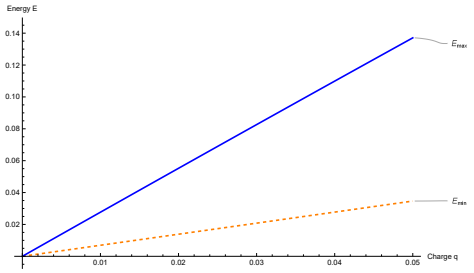
The negative root $\rho_1 = -0.500125$ is discarded immediately, as radial geometric coordinates satisfy the strict physical constraint $\rho > 0$. The two positive roots ρ_2 and ρ_3 both satisfy $F'(\rho) = 0$, each corresponding to a candidate extremal radius for some mass M with $\rho_2 < \rho_3$. Notice that ρ_2 corresponds only to a root of $F'(\rho) = 0$ and does not represent a physical horizon of the black hole under consideration. Since a physical observer can only remain outside the horizon, we consider $\rho_e = \rho_3$ hereafter.

Substituting the outer horizon radius $\rho_+ = \rho_e = \rho_3 = 0.499875$ into Eq. (7), we have

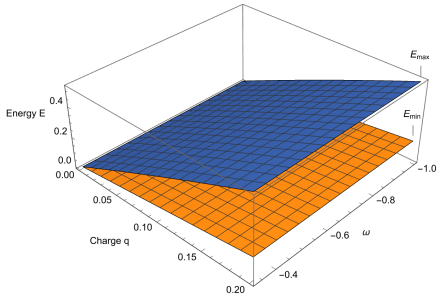
$$E_{\min} = 0.693397q. \tag{13}$$

Substituting our fixed geometric and quintessence coupling constants into Eq. (10) and taking the horizon as $\rho_e = 0.499875$ and mass $M_e = 2.38529$, we obtain

$$\begin{aligned} E_{\max} &= \frac{\rho_e^2}{l^2} - 2(b+q)^2 \ln \rho_e - \frac{\alpha}{\rho_e^{2(\omega+1)}} - M_e \\ &= \frac{0.499875^2}{l^2} - 2(b+q)^2 \ln 0.499875 - \frac{\alpha}{0.499875^{2(\omega+1)}} - 2.38529. \end{aligned} \tag{14}$$



(a) Plot of E-q curves with $\omega = -0.5$. The solid line is $E_{\max}$, the dashed line is $E_{\min}$. It is easy to find the proper charge q which satisfies the $E_{\min} < E < E_{\max}$.



(b) Plot of E-q-ω. The upper surface corresponds to $E_{\max}$, and the lower one corresponds to $E_{\min}$. It is easy to get the proper charge q under different ω satisfy $-1 < \omega < -\frac{1}{3}$.

Figure 1: Energy-charge relation illustrating the formal overcharge window. One could easily find the proper parameters satisfying $E_{\min} < E < E_{\max}$ where full particle absorption mathematically eliminates all real event horizons.

With the same parameter value $b = 1$, $\alpha = 0.0005$, $l = 0.5$, $\omega = -0.5$, we obtain the plot of energy E with charge q shown in Fig. 1a. It is clear that one could easily find the proper charge q which satisfies $E_{\min} < E < E_{\max}$. As we have chosen $b = 1$, we now choose $q = 0.001 \ll b$ as the test particle's charge.

To verify that a valid overcharge window $E_{\min} < E_{\max}$ exists for all physically admissible quintessence state parameters $-1 < \omega < -\frac{1}{3}$, we obtain the explicit charge-dependent expression for maximal overcharge energy with arbitrary state parameter ω as

$$E_{\max} = -0.0005 \times 0.499875^{-2(\omega+1)} + 1.38679(q+1)^2 - 1.38579 \qquad (15)$$

Figure 1b shows different ω located in $-1 < \omega < -\frac{1}{3}$. The upper surface corresponds to $E_{\max}$, and the lower one corresponds to $E_{\min}$. It is easy to see that we can always find a suitable charge q for different values of ω. For simplicity, we choose $\omega = -0.5$. This value lies centrally within the standard quintessence bound $-1 < \omega < -\frac{1}{3}$ and provides a simple representative case for detailed geometric and dynamical analysis.

4 Numerical horizon solving and post-acquisition spacetime evaluation

We now discuss the full absorption of a charged test particle with energy falling within the formal overcharge window $E_{\min} < E < E_{\max}$ and evaluate the post-acquisition radial metric function $F_{\text{after}}(\rho)$ across all positive radial coordinates.

We still choose $b = 1$, $l = 0.5$, $\alpha = 0.0005$ and take $q = 0.001$. For the unfixed ω, we obtain the plot for different values of ω in Fig. 2. The flat 0 reference surface sits entirely below the curved one, indicating no positive real roots exist for any valid quintessence state parameter.

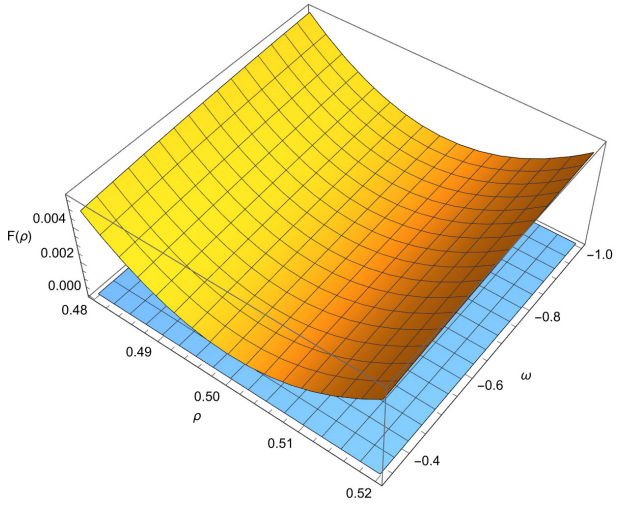


Figure 2: Plot of $F_{\text{after}}(\rho)$ as a function of ρ and ω. The flat 0 reference surface sits entirely below the curved one, indicating no positive real roots exist for any valid quintessence state parameter.

Thus, we still adopt the fixed representative quintessence state parameter $\omega = -0.5$. We obtain $E_{\min} = 0.000693397$ and $E_{\max} = 0.00277498$. The proper energy E satisfies $E \ll M_e$. We now choose $m = E = 0.001$ for simplicity.

Based on the parameters $b = 1$, $l = 0.5$, $\alpha = 0.0005$, $q = 0.001$, $\omega = -0.5$ and $m = E = 0.001$, we obtain the plot of $F(\rho)$ with ρ shown in Fig. 3. The curved line is above the zero axis, indicating the absence of positive real radial roots.

Algebraic root-finding applied to $F(\rho) = 0$ yields only complex imaginary solutions, with no positive real geometric horizons to cloak the central

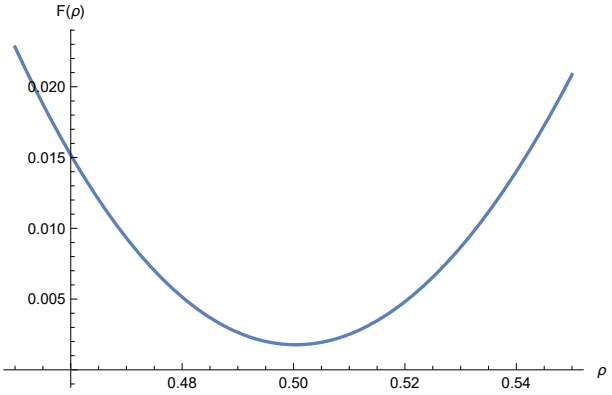


Figure 3: Two-dimensional slice of $F_{\text{after}}(\rho)$ for fixed $\omega = -0.5$, verifying no real radial zeros.

spacetime singularity. The numerically computed complex outer horizon root representative of all post-acquisition algebraic solutions reads

$$\rho_{+(\text{after})} = 0.500301 + i0.0148896. \tag{16}$$

Complex radial roots possess no geometric representation, indicating the formation of a naked curvature singularity observable to distant asymptotic observers if the test particle successfully crosses the outer horizon. In Section 5, we demonstrate that an exterior potential barrier prevents low-energy particles from penetrating the horizon surface, dynamically suppressing this potential WCCC violation scenario despite the existence of a formal overcharge energy window.

5 Radial effective potential and exterior repulsive barrier protection

We start from the full covariant conserved energy equation for massive charged test particles with purely radial motion $\dot{\phi} = 0$:

$$E = -qb \ln \rho + \sqrt{m^2 F(\rho) \left(1 + \frac{\dot{\rho}^2}{F(\rho)}\right)}. \tag{17}$$

Rearranging to isolate the radial kinetic term $\dot{\rho}^2$:

$$\dot{\rho}^2 = \frac{\left(E + qb \ln \rho\right)^2}{m^2} - F(\rho). \tag{18}$$

We use the standard effective potential definition $\dot{\rho}^2 + V_{\text{eff}}(\rho) = 0$, which gives the global radial effective potential valid for all $\rho > 0$:

$$V_{\text{eff}}(\rho) = -\dot{\rho}^2 = F(\rho) - \frac{\left(E + qb\ln\rho\right)^2}{m^2}. \tag{19}$$

Substituting Eq. (2), we have

$$V_{\text{eff}}(\rho) = -\alpha\rho^{-2(\omega+1)} - 2b^2\ln(\rho) - \frac{\left(bq\ln(\rho) + E\right)^2}{m^2} + \frac{\rho^2}{l^2} - M, \tag{20}$$

Here the mass parameter M is identified with the pre-absorption extremal mass, $M = M_e$, because the effective potential governs the motion of the test particle before it is absorbed; the post-absorption quantities introduced in Section 4 do not enter this construction.

Taking $b = 1$, $l = 0.5$, $\alpha = 0.0005$, $q = 0.001$, $\omega = -0.5$ and $m = E = 0.001$, we obtain Fig. 4.

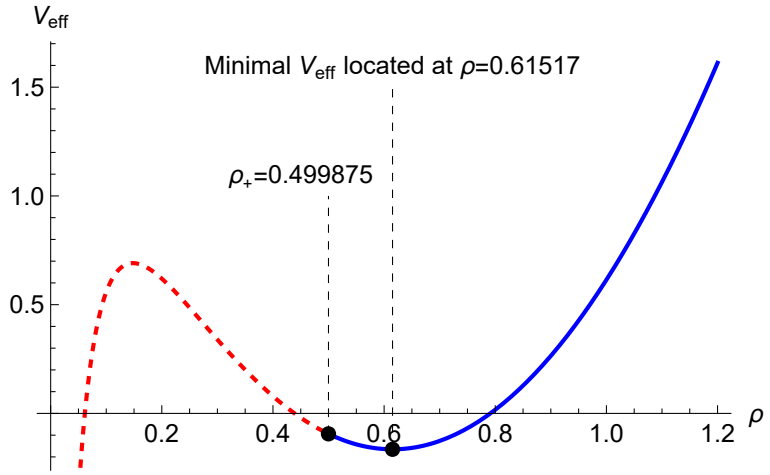


Figure 4: Radial effective potential $V_{\text{eff}}(\rho)$ for a charged test particle. The vertical dashed line marks the outer horizon location $\rho_+ = \rho_e = 0.499875$. The solid curve covers the physical exterior domain $\rho > \rho_+$, while the dashed curve traces the interior region $\rho < \rho_+$. The minimum of the effective potential occurs at $\rho_{\text{VeffMin}} = 0.61517$, which lies strictly outside the event horizon, confirming that the repulsive barrier shields the black hole against overcharging.

The solid portion of the potential curve represents the physical exterior domain $\rho > \rho_+$, while the dashed portion corresponds to the interior region $\rho < \rho_+$. The vertical dashed line at $\rho = \rho_+$ provides a direct visual reference.

The minimum of the effective potential is located at $\rho_{\text{VeffMin}} = 0.592010$ by solving $\frac{dV_{\text{eff}}}{d\rho} = 0$, which satisfies $\rho_{\text{VeffMin}} > \rho_+$, confirming that the relevant extremum lies strictly in the exterior spacetime. As ρ approaches ρ_+, the potential rises from this exterior minimum, forming a repulsive barrier.

For our benchmark particle energy value $E = m = 0.001$, which falls within the formal overcharge window $E_{\text{min}} < E < E_{\text{max}}$, as the particle moves radially inward from spatial infinity and crosses ρ_{VeffMin}, the effective potential rises monotonically, forming a continuously increasing outward repulsion. Since the particle's conserved energy E is lower than the potential values encountered on the horizon side of the minimum, it cannot overcome this outward rise and is scattered back before reaching the horizon. Full accretion therefore cannot physically occur. The fact that the effective potential minimum resides outside the horizon thus acts as an inherent dynamical protection mechanism for the WCCC. Consequently, any particle with energy in the formal overcharge window $E_{\text{min}} < E < E_{\text{max}}$ cannot reach the horizon, and the black hole is protected by quintessence.

6 Parameter-dependence of the quintessence shielding mechanism

In the preceding sections, we demonstrated that for a representative benchmark parameter set $b = 1$, $l = 0.5$, $\alpha = 0.0005$, $\omega = -0.5$ and test-particle charge $q = 0.001$, a potential barrier located outside the outer horizon prevents charged test particles inside the formal overcharging window $E_{\text{min}} < E < E_{\text{max}}$ from reaching the event horizon. The WCCC is thereby dynamically protected by the surrounding quintessence fluid. In order to check whether this protective effect a generic feature for all physically reasonable parameters, or merely a numerical coincidence restricted to our particular choice of benchmark parameters, we perform systematic multi-dimensional parameter scans over the quintessence coupling strength α, the AdS curvature scale l, the black-hole electromagnetic coupling b, and the quintessence state parameter ω. For each parameter set, we evaluate the outer horizon radius ρ_+, the extremal mass M_e, the energy thresholds E_{min} and E_{max}, and the representative particle energy $m = E$ taken as the mid-point $(E_{\text{min}} + E_{\text{max}})/2$ inside the formal overcharging window. We then compute the radial location of the minimum of the effective potential ρ_{VeffMin}, and monitor the ratio $\rho_{\text{VeffMin}}/\rho_+$. $\rho_{\text{VeffMin}}/\rho_+ > 1$ indicates that the relevant extremum of the effective potential lies in the physical exterior domain of the spacetime, the black hole could be protected.

We first vary the quintessence coupling strength α while keeping the remaining parameters fixed at $b = 1$, $l = 0.5$, $\omega = -0.5$, and $q = 0.001$. The coupling α quantifies the strength of the quintessence dark energy correction. We select four values $\alpha = \{0.0001, 0.0002, 0.0003, 0.0004\}$, all satisfying the weak-perturbation condition $\alpha \ll 1$ required for astrophysical consistency. Numerical results are summarized in Table 1.

Table 1: Numerical results for varying quintessence coupling α. All entries are computed from numerical data for presentation.

α	ρ_+	M_e	$E_{\min}$	$E_{\max}$	$m = E$	$\rho_{+(\text{after})}$	ρ_{VeffMin}	$\frac{\rho_{\text{VeffMin}}}{\rho_+}$
0.0001	0.499975	2.38609	0.000693197	0.00277418	0.00173369	$0.500432 + i0.0113941$	0.592107	1.18427
0.0002	0.49995	2.38589	0.000693247	0.00277438	0.00173381	$0.500407 + i0.0113948$	0.592082	1.18428
0.0003	0.499925	2.38569	0.000693297	0.00277458	0.00173394	$0.500382 + i0.0113955$	0.592058	1.18429
0.0004	0.4999	2.38549	0.000693347	0.00277478	0.00173406	$0.500357 + i0.0113962$	0.592034	1.18431

As α increases, the extremal horizon radius ρ_+ decreases slightly while the extremal mass M_e drops, and the ratio $\rho_{\text{VeffMin}}/\rho_+$ remains consistently above 1.18, confirming that the effective potential barrier stays well outside the horizon for all sampled α. The post-accretion complex roots $\rho_{+(\text{after})}$ indicate that horizon disappearance would occur algebraically if the particle reached the horizon, but the exterior barrier prevents this from happening dynamically. These results show that stronger quintessence coupling reinforces the shielding mechanism, while even the smallest sampled $\alpha = 0.0001$ still provides an exterior barrier.

We next vary the AdS curvature radius l to examine the influence of spacetime asymptotic curvature on the shielding effect. The parameters are fixed at $b = 1$, $\alpha = 0.0005$, $\omega = -0.5$, and $q = 0.001$. Four representative values $l = \{0.3, 0.4, 0.6, 0.7\}$ are chosen to cover both more strongly curved ($l < 0.5$) and less curved ($l > 0.5$) AdS backgrounds. Results are listed in Table 2.

Table 2: Numerical results for varying AdS curvature scale l.

l	ρ_+	M_e	$E_{\min}$	$E_{\max}$	$m = E$	$\rho_{+(\text{after})}$	ρ_{VeffMin}	$\frac{\rho_{\text{VeffMin}}}{\rho_+}$
0.3	0.299875	3.40628	0.00120439	0.00481997	0.00301218	$0.30013 + i0.00901678$	0.329862	1.1
0.4	0.399875	2.83133	0.000916603	0.00366825	0.00229243	$0.400229 + i0.0104856$	0.453463	1.13401
0.6	0.599875	2.02082	0.000511034	0.00204516	0.0012781	$0.600437 + i0.0117365$	0.762814	1.27162
0.7	0.699875	1.71264	0.000356854	0.00142813	0.000892491	$0.700544 + i0.0114354$	1.02739	1.46796

As l increases, the horizon radius ρ_+ grows and the extremal mass M_e decreases. The ratio $\rho_{\text{VeffMin}}/\rho_+$ increases monotonically from 1.10 at $l = 0.3$ to 1.47 at $l = 0.7$. This indicates that larger AdS curvature radius (weaker asymptotic curvature) pushes the barrier further outside the horizon. Even

at the smallest scanned $l = 0.3$, the ratio remains above unity, so the shielding mechanism operates across the entire scanned range. The post-accretion complex roots confirm that horizon destruction would be the algebraic outcome of successful accretion at all l values, reinforcing the necessity of the dynamical barrier interpretation.

Next, we scan over black-hole electromagnetic coupling b. The parameter b controls the intrinsic charge of the Peldan black hole. We fix $\alpha = 0.0005$, $l = 0.5$, $\omega = -0.5$, and $q = 0.001$, and take four values $b = \{0.6, 0.8, 1.2, 1.4\}$. Table 3 reports the results.

Table 3: Numerical results for varying black-hole electromagnetic coupling b.

b	ρ_+	M_e	$E_{\min}$	$E_{\max}$	$m = E$	$\rho_{+(\text{after})}$	ρ_{VeffMin}	$\frac{\rho_{\text{VeffMin}}}{\rho_+}$
0.6	0.299652	1.22519	0.00072308	0.00289473	0.0018089	$0.300078 + i0.0116472$	0.38253	1.27658
0.8	0.399805	1.8116	0.000733424	0.00293553	0.00183448	$0.400248 + i0.0117244$	0.484157	1.21098
1.2	0.599913	2.91034	0.000613164	0.00245368	0.00153342	$0.600381 + i0.0107146$	0.709183	1.18214
1.4	0.699936	3.35745	0.000499472	0.0019986	0.00124904	$0.700414 + i0.00966727$	0.847437	1.21073

As b increases, the horizon radius ρ_+ grows and the extremal mass M_e rises. The barrier ratio $\rho_{\text{VeffMin}}/\rho_+$ remains above 1.18 for all sampled b, with a shallow minimum near $b = 1.2$. The post-accretion complex roots again confirm algebraic horizon disappearance. Within the test-particle regime $q \ll b$, the shielding mechanism is robust against variations in the black hole's intrinsic charge.

Finally, we scan the quintessence equation-of-state parameter ω over the physical interval $-1 < \omega < -1/3$. We fix $b = 1$, $l = 0.5$, $\alpha = 0.0005$, and $q = 0.001$ and select four values of $\omega = \{-0.4, -0.6, -0.7, -0.8\}$. Note that the benchmark $\omega = -0.5$ is not listed separately here because it was already established as the reference case in the main text. Results are given in Table 4.

Table 4: Numerical results for varying quintessence state parameter ω.

ω	ρ_+	M_e	$E_{\min}$	$E_{\max}$	$m = E$	$\rho_{+(\text{after})}$	ρ_{VeffMin}	$\frac{\rho_{\text{VeffMin}}}{\rho_+}$
-0.4	0.5	2.38515	0.000693147	0.00277398	0.00173356	$0.500285 + i0.011402$	0.591996	1.18399
-0.6	0.5	2.38542	0.000693147	0.00277398	0.00173356	$0.50037 + i0.0113977$	0.592058	1.18412
-0.7	0.499943	2.38554	0.000693261	0.00277443	0.00173385	$0.5004 + i0.0113947$	0.592073	1.18428
-0.8	0.5	2.38563	0.000693147	0.00277398	0.00173356	$0.500424 + i0.0113949$	0.592101	1.1842

Across the scanned ω range, the barrier ratio stays above 1.18, confirming that the exterior repulsive barrier persists for all physically admissible quintessence state parameters. The extremal mass M_e and horizon radius ρ_+ exhibit only minor variations, indicating that the shielding mechanism is not strongly sensitive to the precise value of ω within its allowed range. This

complements the main-text result at $\omega = -0.5$ and demonstrates that the quintessence protection is a generic feature of the entire physical parameter domain.

The parameter scans presented above extend the benchmark result of Section 5 to a broader region of the parameter space. In every case, $\rho_{\mathrm{VeffMin}} > \rho_+$ is always valid, confirming that the relevant extremum of the effective potential lies outside the outer horizon, in the physical exterior domain. This geometric fact, combined with the algebraic post-accretion complex roots, establishes a consistent physical picture: although the formal energy window $E_{\min} < E < E_{\max}$ permits horizon destruction in principle, the exterior repulsive barrier dynamically forbids the required particle infall. The shielding effect of quintessence is therefore not an artifact of a particular parameter choice but a robust feature of the Peldan-quintessence system within the physically motivated parameter ranges explored here.

7 Summary

In this paper, we perform comprehensive analytical and numerical examinations of the weak cosmic censorship conjecture (WCCC) for $(2 + 1)$-dimensional Peldan black holes surrounded by quintessence. We find that the radial effective potential exhibits an obvious repulsive barrier outside the outer horizon. Low-energy in-falling particles cannot cross this barrier and the event horizon is preserved. This protective barrier originates from the quintessence correction term.

To confirm this result, we have performed multi-dimensional parameter scans over the quintessence coupling strength α, the AdS curvature scale l, the black-hole electromagnetic coupling b, and the quintessence state parameter ω. In every case examined, the relevant extremum of the effective potential lies outside the outer horizon, confirming that the repulsive barrier dynamically forbids horizon-destroying particle infall throughout the physically motivated parameter ranges.

Our result coincides with the conclusion of previous work on RN-Q black holes[11]. Quintessence fluid generates an exterior potential barrier that shields black holes against overcharge-induced naked singularities. Our results further verify that such a protective mechanism also holds for logarithmic $(2 + 1)$ Peldan geometries, within the parameter ranges considered, demonstrating quintessence's shielding effect on charged black hole backgrounds. This also indicates that there are more aspects of the quintessence model to explore.

In future work, we plan to consider angular momentum-bearing spin-

ning test particles to break the pure radial in-fall restriction to examine whether quintessence can provide analogous potential barrier protection in those spacetimes with angular momentum, or constructing dynamic Vaidya-type accretion geometries to replace static instantaneous particle absorption.

Acknowledgments

We thank Dr.Zhang and Prof.Wu for valuable comments and enlightening discussions. This work was supported by "Special Project of Education Department of Shaanxi Province in Natural Science" with grant number 20JK0635. This work is also supported by "Talent Foundation" of Weinan Normal University with grant number 201120039.

References

[1] Penrose R 2002 *Gen. Relativ. Gravit.* **34** 1141

[2] Sorce J and Wald R M 2017 *Phys. Rev. D* **96** 104014

[3] Hubeny V E 1998 *Phys. Rev. D* **59** 064013

[4] Düztaş K 2019 *Eur. Phys. J. C* **79** 316

[5] Zhang Y and Gao S 2014 *Int. J. Mod. Phys. D* **23** 1450044

[6] Gao S and Zhang Y 2013 *Phys. Rev. D* **87** 044028

[7] Siahaan H M 2016 *Phys. Rev. D* **93** 064028

[8] Kiselev V V 2003 *Class. Quantum Grav.* **20** 1187

[9] Qu Y, Tao J and Wu J 2022 *Eur. Phys. J. C* **82** 10120

[10] Hong W, Mu B and Tao J 2019 *Nucl. Phys. B* **949** 114826

[11] Tang H and Zhang J 2023 *Chin. Phys. B* **32** 120402

[12] Tongzheng Wang et al 2025 *Chin. Phys. B* **34** 030401

[13] Siyu Jian et al 2024 *Chin. Phys. B* **33** 100504

[14] Bañados M, Henneaux M, Teitelboim C and Zanelli J 1993 *Phys. Rev. D* **48** 1506

[15] Das S, Majumdar P and Bhaduri R K 2002 *Class. Quantum Grav.* **19** 2355

[16] Tang H, Song Y, Yue R-H and Sun C-Y 2017 *Chin. Phys. Lett.* **34** 040401

[17] de Oliveira J and Fontana R D B 2018 *Phys. Rev. D* **98** 044005

[18] Saleh M, Thomas B B and Kofane T C 2009 *Chin. Phys. Lett.* **26** 109802